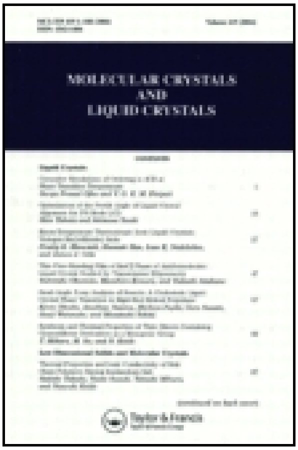

Molecular Crystals and Liquid Crystals

Publication details, including instructions for authors and subscription information:
http://www.tandfonline.com/loi/gmcl20

Influence of the Surfaces on the Nucleation Process During the Cholesteric-Nematic Transition

Andriy Kozachenko [a] & Lachezar Komitov [a]

[a] Department of Physics, Chalmers University of Technology and Göteborg University, Göteborg, Sweden

Version of record first published: 18 Oct 2010

To cite this article: Andriy Kozachenko & Lachezar Komitov (2004): Influence of the Surfaces on the Nucleation Process During the Cholesteric-Nematic Transition, Molecular Crystals and Liquid Crystals, 412:1, 205-217

To link to this article: http://dx.doi.org/10.1080/15421400490439833

Mol. Cryst. Liq. Cryst., Vol. 412, pp. 205/[1815]–217/[1827], 2004
Copyright © Taylor & Francis Inc.
ISSN: 1542-1406 print/1563-5287 online
DOI: 10.1080/15421400490439833

INFLUENCE OF THE SURFACES ON THE NUCLEATION PROCESS DURING THE CHOLESTERIC-NEMATIC TRANSITION

Andriy G. Kozachenko[§] *and Lachezar Komitov*[*]
Department of Physics, Chalmers University of Technology and Göteborg University, Göteborg SE-41296, Sweden

The nucleation phenomenon in short pitch cholesteric liquid crystals (LC), taking place during the relaxation from the electric field-induced cholesteric-nematic (CN) transition, has been investigated for various boundary conditions. The dynamic hysteresis properties have been studied by direct optical methods. For the first time it is shown the strong evidence that the nucleation is not exceptionally a bulk phenomenon and the supporting solid surfaces may act as nucleation sites. It is confirmed also that the nucleation velocity is not a function of the type of molecular alignment at the liquid crystal/solid interface rather than it depends on the uniformity of the surface interactions with liquid crystal molecules. This result is of importance for time scale optimization in modern fast driving schemes for cholesteric LCDs.

Keywords: cholesteric liquid crystals; hysteresis; nucleation; surface

INTRODUCTION

Due to the bistability and intrinsic memory, cholesteric liquid crystals remain in the scope of interest for display applications. During the last decade the interest in the display applications of cholesterics has been renewed due to the progress in the material science that made possible the so-called short pitch cholesteric display modes to become compatible with the moderate voltage driving electronics. Short pitch cholesterics are very attractive because of their unique optical properties as the selective

---

The authors are gratefully expressing their acknowledge to professors Dr. Yu. Reznikov and Dr. L. A. Kutulya for helpful discussions on this study as well as to Mr. P. Tytarenko for his assistance in cell preparation. The authors would like to acknowledge the financial support given by INTAS.

[§] Permanent address: Kyiv National University for Technology & Design, UA-01011 Kyiv, Ukraine; E-mail: kozachen@i.kiev.ua

[*] Corresponding author. E-mail: komitov@fy.chalmers.se

light reflection that, in fact, could be combined with the texture bistability properties provided that appropriate boundary conditions are present. The twisted configuration of molecular ordering in cholesteric LC can be unwound, i.e. transformed into nematic configuration, by applying an external electric field due to the dielectric coupling. This kind of transition was described by de Gennes [1]. One of the most important features of the cholesteric-nematic transition effect that make short pitch cholesterics very attractive is the hysteresis behaviour. Otsuka *et al.* [2,3], Walter and Kruger [4] and Greubel [5] reported that during the relaxation from the unwound state to the helical molecular ordering, the field-induced nematic state can be saved even below the cholesteric-nematic transition threshold. Greubel also reported that for the homeotropic alignment at the supporting solid surface, the inhomogeneities like surface and bulk defects might strongly influence the hysteresis properties. Kashnow *et al.* [6] were the first to suppose the reverse nematic to cholesteric transition to be a nucleation process, which, in fact, occurs around defect sites for homeotropic boundary samples, whereas the entire supporting solid surface may act as a nucleation site for planar boundary conditions. Kawachi and Kogure [7] investigated the nematic-cholesteric (NC) relaxation in long pitch cholesterics and observed the hysteresis irrespective of the boundary conditions. They gave also the evidence that the reverse nematic-cholesteric transition is a nucleation process, which occurs around the bulk and surface defects and concluded that the nucleation velocity does not depend on the type of molecular alignment at the interface, i.e. the nucleation is an exceptionally bulk phenomenon. However, the relaxation process from the field-induced nematic state is still not well understood and requires further investigations. In our previous studies we have found that the type of molecular alignment at the interface (homeotropic or planar) does not, in fact, play a significant role in the nucleation process. Moreover, the nucleation appears to be not only a bulk phenomenon since at appropriate boundary conditions it may be governed by the boundary conditions too [8,9]. This result seems to be very important for the time scale optimization in modern fast driving schemes for cholesteric LCDs because it allows to curtail significantly the row addressing time just by selection of the appropriate boundaries.

In this paper we report the results of our investigations on the influence of the boundary conditions on the nucleation phenomenon in short pitch cholesteric liquid crystals. These results show a strong evidence that the entire confining solid surface may give rise to a nucleation process.

Because of the Bragg selective light reflection properties of short pitch cholesteric texture, it is possible to inspect separately the molecular configuration in the bulk and at the solid surface by means of optical birefringence and selective reflectance measurement techniques. So, if the nucleation process is not influenced by the boundary conditions, the molecular configuration in the bulk and at the solid surface should be quite similar. As a consequence, no significant temporal stratification between evolution kinetics in the bulk and at the solid surface should be observed. On the other hand it is well known that the nucleation occurs around the bulk and surface defects, where the symmetry is broken. These defects act as nucleation seeds if the surface treatments induce an uniform alignment and the typical distance between the neighboring nucleation sites is at least an order of magnitude bigger than the cell thickness [7]. Consequently, if one can suppose that the nucleation is exceptionally a bulk process and their velocity depends only on concentration of the nucleation centers, the small variation of cell thickness should have no effect on the nucleation speed. Otherwise the re-appearance of the helical molecular order should be influenced by the surface.

In order to clarify the evolution dynamics of the unwound cholesteric texture and to prove the assumption that the boundary conditions may play an important role in the nucleation process, we performed a series of experiments with substrates whose surfaces were differently treated. The surface treatment differs not only by the kind of imposed alignment but also by its uniformity and anchoring strength.

THEORY

The experimental results indicate unambiguously that for the real samples the boundary conditions play an important role especially for low d/P_o (cell thickness to quiescent helical pitch) ratio. The liquid crystal/solid surface interactions could even be so strong that they may induce unwinding of the molecular helical order. The anchoring strength is naturally reflected on the values of critical fields associated with texture transitions in cholesterics calculated by *Kawachi* and *Kogure* [7]. They used a pictorial representation in which the threshold fields appear as crossovers of the field-dependent free energy curves for the relevant states in cholesterics: planar, focal conic and induced nematic. This approach was further developed by *Van Sprang* and *Van de Venne* [10] including the liquid crystal/surface interactions. According to their description, the threshold fields are now the crossovers of total free energy curves in an applied electric field and differ from those of *Kawachi* and *Kogure* by incorporation of surface free energy terms. The derived expressions for critical fields in this case are the following:

$$E_{cn} = 2\sqrt{2}\left[\left(\frac{\pi}{P_o}\right)^2\left(\frac{K_{22}}{\varepsilon_o\Delta\varepsilon}\right) + \left(\frac{F_{sn} - F_{sc}}{\varepsilon_o\Delta\varepsilon d}\right)\right]^{1/2} \tag{1}$$

$$E_{nc} = \frac{\pi}{P_o}\left[\frac{4K_{22}^2 - [K_{33}(P_o/d)]^2}{\varepsilon_o \Delta\varepsilon K_{33}} + \frac{4P_o^2 F_{sn}}{\pi^2 d \varepsilon_o \Delta\varepsilon}\right]^{1/2} \tag{2}$$

$$E_{c'c} = 2\sqrt{2}\left[\frac{F_{sn} - F_{sc'}}{\varepsilon_o \Delta\varepsilon d}\right]^{1/2} \tag{3}$$

where E_{cn}, E_{nc}, $E_{c'c}$ - are the critical fields for cholesteric-nematic (CN) transition, reverse nematic-cholesteric (NC) transition and for focal conic deformation, respectively. $F_{sc'}$, F_{sc}, F_{sn} - are the densities of surface free energy in the planar, focal conic and induced nematic states respectively, d - is the cell thickness, K_{22}, K_{33} - are the Frank splay and bend elastic constants, respectively, and $\Delta\varepsilon$ is the dielectric anisotropy of the liquid crystal. Expressions (1–3) were derived assuming that for planar anchoring conditions $F_{sc'} = 0$ and for homeotropic $F_{sn} = 0$.

EXPERIMENT

The investigations have been performed with a variety of aligning layers that provide different director configurations of the cholesteric liquid crystal at the liquid crystal/solid surface interface. The cell preparation has been performed in the following way. Standard glass plates, precoated with ITO conducting electrode, were covered by electron beam evaporated SiO_2–Al_2O_3–SiO_2 dielectric protective layer to avoid the electric shortage. The overall layer thickness was controlled by means of interferometric technique and was kept in the range of 220 nm. Then, an aligning layer was deposited onto the protecting layer. Four differently prepared and treated aligning layers were investigated in our experiments namely Polyimide (PI) AD-9103 (Ukraine), Octadecyl-trichlorosilane (OTS) and Silicon Oxide SiO_x, respectively. Polyimide film was spin coated, dried and imidized. When no additional treatment is applied it provides a degenerate planar orientation of the liquid crystal molecules at the solid surface. After unidirectional mechanical rubbing, the polyimide layer provides homogeneous planar alignment. Octadecyltrichlorosilane (OTS) film, promoting a homeotropic alignment of the liquid crystal molecules, was deposited onto the protected layer by dipping. SiO_x alignment layer, obliquely deposited by cathode reactive sputtering in glow discharge plasma, provided a planar alignment with low pretilt of the molecules at the substrate surface. After the deposition of the alignment layers, the cells were assembled and then filled with the liquid crystals in a vacuum chamber.

Cholesteric liquid crystal used in our experiment was a mixture of cholesterol derivatives CH12-M (Ukraine) which was added to the nematic host E7 (BDH Ltd.) in ratio 3:2 by weight. The resulting mixture has a temperature independent helical pitch $P_o \approx 0{,}33\,\mu\text{m}$ and corresponding wavelength of maximum selective reflection from Grandjean texture observed in the region of green light $\lambda_m = 540\,\text{nm}$ at normal light incidence. The dielectric anisotropy of liquid crystal material was measured by means of the dielectric spectroscopy technique to be $\Delta\varepsilon = +2{,}6$.

The procedure for calculation of the surface free energy terms with our liquid crystal material and alignment layers is discussed in details in [9]. Here, we only show their values, which are collected in Table 1.

The dynamic hysteresis properties were determined by means of the experimental setup, which is represented schematically in Figure 1a. It consists of a light source (LS), collimator (C), polarizing microscope (M) with photomultiplier/spectrophotometer (PM), which is embedded into a trinocular system, analog to digital and digital to analog converter (ADC/DAC) and personal computer (PC). The resulting signal of the rectangular form simulated by PC is passing through the DAC and applied to the cell. Any changes in the transmission or in the selective reflection of light are detected by photomultiplier and returned in a digital form to the computer via ADC.

The dynamic hysteresis measurements were carried out using the conventional technique with some modification. First an electric field, higher than critical field for CN transition E_{cn}, is applied to unwind the cholesteric helix. Then the applied field is reduced to a bias field $E_b < E_{cn}$. The time of bias field action T_b, which is one of the parameters in the dynamic response, was fixed for every hysteresis curve. Peculiarity of the experiment lies in the very fact that the electric field was reduced from E_{cn} to E_b not gradually, as in the usual case of quasi-static hysteresis measurements, but stepwise as shown in Figure 1b. In this case, the transitions homeotropic to planar and homeotropic to focal conic textures start to compete with each other as soon as the bias field is settled. So, the final configuration of the cholesteric liquid crystal depends mostly on the duration time of the bias pulse [7]. For our experiments the most interesting sites are the ones, at which competition between the relaxation modes is strongest, i.e. in the vicinity of jump, where the growth and the propagation velocity of focal

TABLE 1 Surface Free Energy Terms for Various Aligning Layers

Alignment layer	$F_{SC'}$, (J/m^2)	F_{SC}, (J/m^2)	F_{SN}, (J/m^2)	Type of alignment
PI, no rubbing	0	$2.9{\cdot}10^{-4}$	$5.5{\cdot}10^{-4}$	Planar, degenerate
PI rubbed	0	$3.2{\cdot}10^{-4}$	$3.9{\cdot}10^{-4}$	Planar, uniform
OTS	$1.8{\cdot}10^{-4}$	$5.4{\cdot}10^{-4}$	0	Homeotropic
SiO$_x$	$2.1{\cdot}10^{-4}$	$4.3{\cdot}10^{-4}$	$7{\cdot}10^{-5}$	Planar, tilted

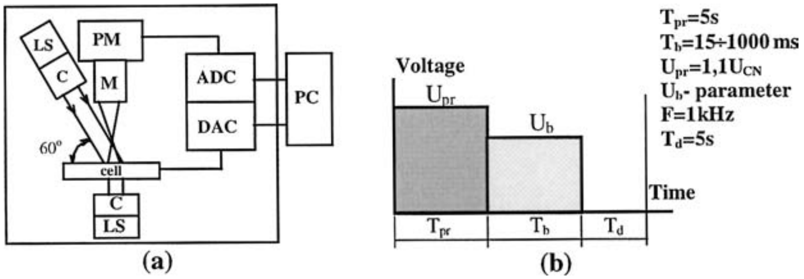

FIGURE 1 Schematic representation of the experimental setup for dynamic hysteresis measurements (a) and sequence of applied voltages (b). (T_d – the delay before the measurements).

conic texture is highest. The variation of the bias pulse duration allows to catch the nucleation onset and to freeze it while bias field is applied. Due to the bistable properties in surface stabilized cholesteric texture, it is easy to distinguish the final state of frozen texture when the field is turned off. The sites with homeotropic configuration will evolve into the planar state whereas the focal conic sites will remain in the same state. The areas occupied by these two textures are easily to be detected by direct optical techniques. The focal conic texture is known to give a contribution into phase delay associated with the optical birefringence as well as it may be identified also by nonselective scattering. The planar state has a strong contribution into a selective reflection and comparatively low one to a phase delay. Finally, the monochromatic light source could be used in order to improve the contrast between these two textures. We must stress here that all investigations have been performed for a high d/P_o ratio. This allows to consider the cholesteric system as stratified anisotropic media which is capable to save the information both at interfacial layers and in the bulk layer separately. The possible configurations of cholesteric textures associated with different boundary conditions in such a layered stratification are schematically depicted on Figure 2.

RESULTS AND DISCUSSION

The major goal of the present study is to investigate the influence of the surface boundary conditions on the nucleation process from the field-induced cholesteric-nematic transition. The surface free energies, calculated for the alignment layers used in our experiments, are given in Table 1 and somewhat differ from the values presented in [10] for similar alignment layers. However, even though similar, the layers used by us for

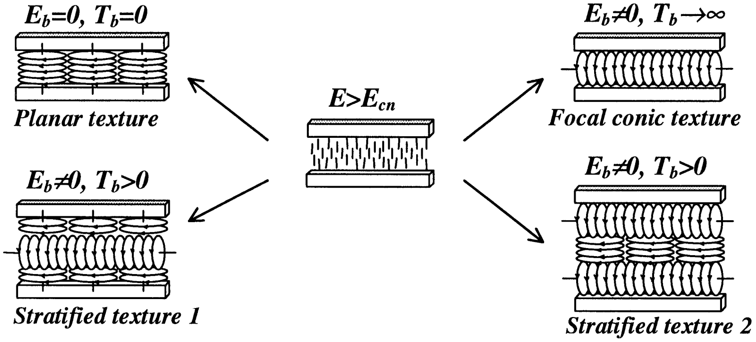

FIGURE 2 Simplified representation of the possible configurations of short pitch cholesteric textures associated with the relaxation from field-induced nematic state. Stratified textures 1&2 represent the cases where the nucleation originates in the bulk and at the surface, respectively.

obtaining planar and homeotropic, respectively, alignment differ substantially from the ones in [10] by their chemical nature as well as by the way of their deposition and, thus, by their structural properties. The noticeable feature which could be seen from Table 1 is that the surface free energy F_{sn} and the threshold field for unwinding of cholesteric helix E_{cn} associated therewith differs for the cells containing the same aligning layers i.e. PI with and without mechanical treatment. It was found that CN transition threshold has diminished after the treatment of polyimide by rubbing and the dynamic hysteresis curves have been significantly modified too [9]. The nucleation time increased at least an order of magnitude after mechanical buffing (see Fig. 3).

If we suppose that the nucleation centers are mostly concentrated at the surface, their density should be drastically diminished after rubbing. In fact, the nucleation seeds are observed very well with polarizing microscopy due to the formation of π-wall circles around the defects, which are existing even above CN threshold. Indeed, these π-walls serve as a powerful source of nucleation but we did not encounter any significant changes in their concentration after rubbing. We have tried to invoke the reasoning of the nucleation theory elaborated by *Van Sprang* [11] and taking into account our experimental results we have concluded that the most likely the nucleation occurs mainly at the surface and then gradually permeates into the bulk for untreated polyimide layers. In order to test our assumption we have investigated the dynamic electro-optical response curves for the same sample with untreated PI layers taken both from the reflectance and transmittance measurement techniques. The respective curves are represented in Figure 4 for the various bias times T_b.

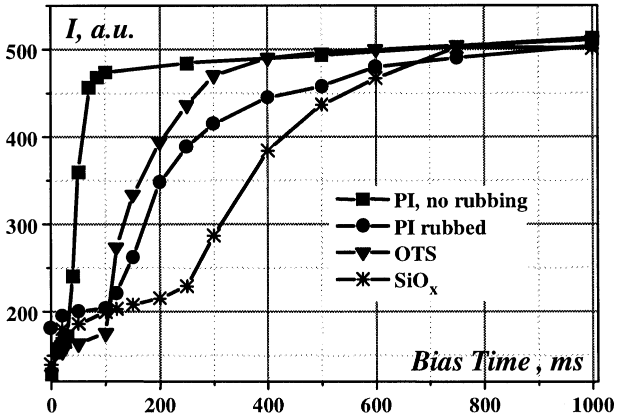

FIGURE 3 Kinetics of the nucleation process in cholesteric samples for various boundary conditions of the same cell thickness $d \approx 4{,}5\,\mu m$ (transmittance mode).

On the sites with maximum nucleation velocity we built up the curves which reflect the dynamic of nucleation process and plotted them as transmittance (reflectance) curves v.s. bias time. These curves are represented in Figure 5. The noticeable feature in these curves is that they show a significant diversity for the nucleation times at the surface and in the bulk. As it could be seen from Figure 5 the nucleation at the bulk is just about to begin whereas the same process has been completed at the surface (no selective reflection). This diversity may, however, be due to the transient processes associated with the smooth deviation of helical axes from the surface normal. It's well known that bend type deformation may also induce the nucleation and corresponding turn of the helical axes. In such manner the selective reflection may not be observed when the helical axes becomes highly tilted, so that the Bragg diffraction conditions are not satisfied. Nonetheless, this experiment at least showed us that for this kind of alignment the nucleation is a continuous process.

The next step is to prove that it occurs at the surface at first and then permeates into bulk. An indication that the nucleation process starts at the solid surface is a strong dependence of the nucleation velocity on the sample thickness. Therefore we investigated the nucleation time as a function of cell thickness. The corresponding light transmission curves of the nucleation velocity for the investigated aligning layers, listed in Table 1, are depicted in Figure 6. These curves, which reflect the dynamics of the nucleation process, are built up on the sites with maximum nucleation velocity, detected by transmittance technique, vs. bias time (see Fig. 4a). As seen, the samples with non-rubbed PI are sensitive to the thickness variations, hence indicating that the nucleation process originates at the

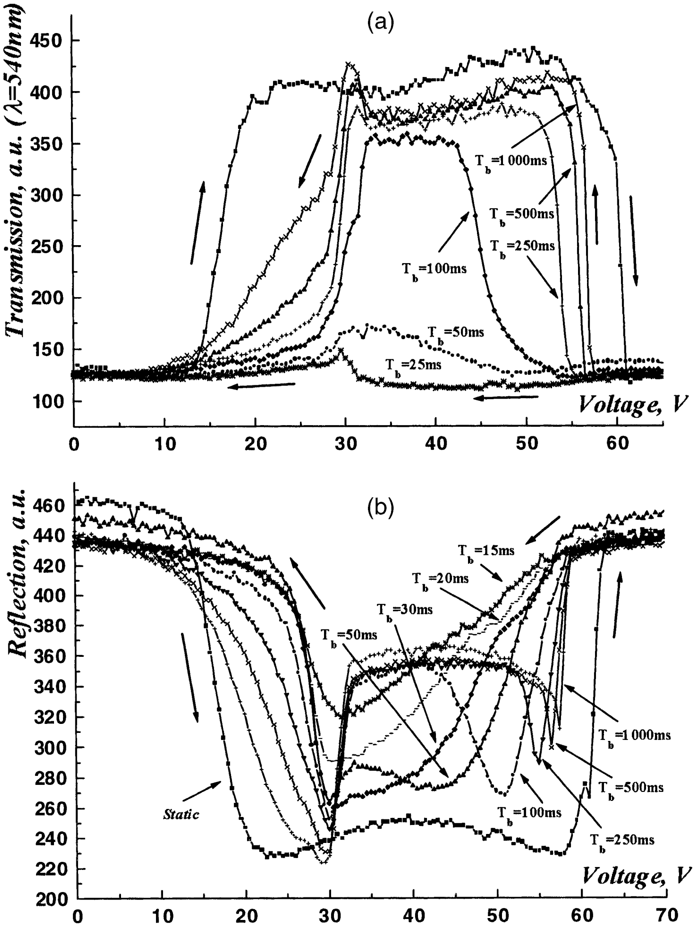

FIGURE 4 Dynamic electrooptical response curves of a cholesteric sample ($d = 6\,\mu\text{m}$) aligned with non-rubbed PI alignment layer obtained by means of the transmission -(a) and reflection -(b) techniques.

solid surface. In the first approach, we have found that the nucleation time in the samples with rubbed PI alignment layer is a linear function of the cell thickness, but further studies are needed to evaluate more precisely the character of this dependence. The samples with rubbed PI and OTS alignment layers, respectively, exhibit nucleation time approximately of the same order of magnitude, which are, in fact, rather insensitive to such variations. Hence, the very fact that the nucleation time is independent on the cell thickness is a clear indication that the nucleation process in these cells is driven by the surface and bulk defects. The longest nucleation time was

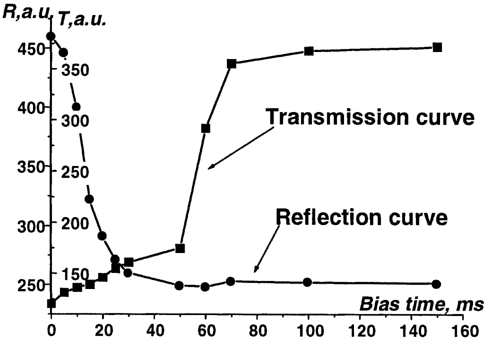

FIGURE 5 Kinetics of the nucleation process in cholesteric sample with non rubbed PI alignment layer obtained by means of transmission and reflection techniques.

measured in the samples with SiO_x alignment layers, which, in fact, also show cell thickness dependence. If compared with the samples with the PI (rubbed as well as non-rubbed) alignment layers, the longer nucleation time in the case of SiO_x layer seems to reflect the lower value of F_{SN} in this

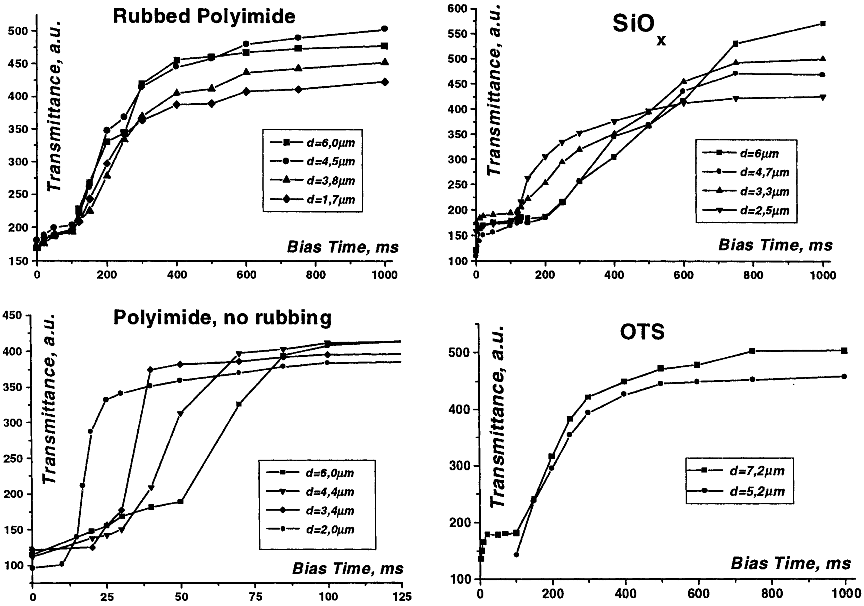

FIGURE 6 Kinetics of nucleation process in cholesteric systems for the various alignment layers and cell thickness. (transmittance mode).

case as well as smaller concentration of defects at the surface. Such an assumption seems to be quite reasonable since the anchoring on SiO_x layer is known to be weaker than the one on PI layers. According to the nucleation theory elaborated by van Sprang and van de Venne [10,11], the birth of cholesteric texture from field induced nematic state takes place at the sites where the symmetry breaks occur. In case of planar alignment, the bend type deformation at the surface may be considered as the initiator of the nucleation onset. Because the concentration of the nucleation centers is small their influence on the thickness dependence of the nucleation time could be considered as small too.

When discussing the possible reason(s) for the beginning of the nucleation process at the solid surfaces in the samples with non-rubbed PI alignment layer and why the process takes place in this case, we certainly should be aware which kind of changes occur after the mechanical treatment of the PI layer.

The non-rubbed PI film consists of randomly distributed clusters of PI molecules [12]. These clusters are of different size and have deformed spherical shapes. Therefore, the topography of the non-rubbed PI film is very irregular. Such film gives random planar alignment, i.e. the preferred direction of alignment varies locally. After the mechanical treatment, the PI film drastically changes. The film topography becomes smoother and long cluster chains as well as a system of shallow and deep groves are formed along the rubbing direction. The rubbing process results in anisotropy of the physical properties of PI films. As a consequence, the rubbed PI films align most of the liquid crystal materials into uniform planar texture. The major feature of the non-rubbed PI alignment layer is the imposed local variation of the liquid crystal director forming a domain structure. One may consider the existence of preferred direction within the single domain only (see Fig. 7). The strong anchoring of the liquid crystal on the PI surface and the variation of the director in the neighboring domains give rise

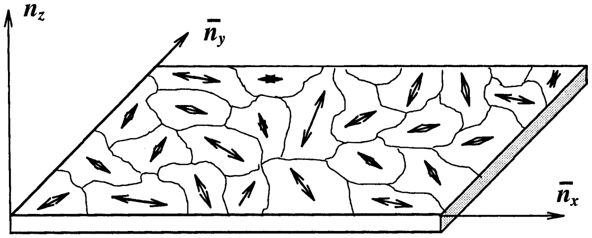

FIGURE 7 Schematic representation of the liquid crystal director distribution imposed by a non-rubbed polyimide film.

to formation of local surface defects. These defects will play the role of nucleation seeds. Because the distance between neighboring defects is rather small (less than 1 μm) if compared to the thickness of LC layer, the nucleation could be considered as driven by the whole surface. Our finding is strongly supported by the observation of surface-induced nucleation reported in [13], where periodic surface boundary conditions resulted in uniform lying helix texture of short pitch cholestertic during the relaxation from field-induced cholesteric-nematic transition.

As mentioned, the nucleation velocity in the case of SiO_x alignment layer was also found to be dependent on the sample thickness, thus indicating that the nucleation process begins at the solid surface. The reduced surface scalar order parameter in this case could be considered as one of the possible reasons. However, further studies of the nucleation process dynamics in samples with SiO_x alignment layers are necessary in order to shed more light on the origin of the surface influence on the nucleation process in this case. Such studies are underway.

CONCLUSION

In this paper we have investigated the nucleation phenomenon in short pitch cholesteric liquid crystal samples during the relaxation process from the field-induced cholesteric to nematic transition for various alignment layers and boundary conditions. We have found that the nucleation is not exceptionally bulk phenomenon, as stated by Kawachi and Kogure [7], it could be largely driven by the liquid crystal/surface interactions. This finding opens the way to increase the nucleation speed at least an order of magnitude just by careful selection of appropriate boundary conditions. This allows to reduce drastically the row addressing time and eventually the total frame time in modern fast driving schemes for cholesteric LCDs.

REFERENCES

[1] de Gennes, P. G. (1968). *Solid State Commun.*, *6*, 163.
[2] Otsuka, T. & Tsukamoto, M. (1973). *Jpn. J. Appl. Phys.*, *12*, 22.
[3] Otsuka, T., Tsukamoto, M., & Tsuchiya, M. (1973). *Jpn. J. Appl. Phys.*, *12*, 371.
[4] Walter, K. H. & Kruger, H. H. (1974). *Ber. Bunsenges. Phys. Chem.*, *78*, 912.
[5] Greubel, W. (1974). *Appl. Phys. Lett.*, *25*, 5.
[6] Kashnov, R. A., Bigelow, J. E., Cole, H. S., & Stein, C. R. (1973). *Liquid Crystals and Ordered Fluids*, Johnson, J. E. & Porter, R. S. (Eds.), Plenum: NY., *4*(II), 483.
[7] Kawachi, M. & Kogure, O. (1977). *Japanese J. of Appl. Phys.*, *16*, 1673.
[8] Kozachenko, A., Oleksenko, P., Sorokin, V., & Nazarenko, V. (1997). *Proc. IDRC'97*, p. 148.
[9] Kozachenko, A. G. (2001). *Mol. Cryst. Liq. Cryst.*, *361*, 149.

[10] van Sprang, H. A. & van de Venne, J. L. M. (1985). *J. Appl. Phys.*, *57*, 175.
[11] van Sprang, H. A. (1985). *Mol. Cryst. Liq. Cryst.*, *122*, 269.
[12] Kim, Y. B., Olin, H., Park, S. Y., Choi, J. W., Komitov, L., Matsuszczyk, M., & Lagerwall, S. T. (1995). *Appl. Phys. Lett.*, *66*, 2218.
[13] Komitov, L., Bryan-Brown, G. P., Wood, E. L., & Smout, A. B. J. (1999). *J. Appl. Phys.*, *86*, 3508.